Research Article

MOLECULAR PAIN

Molecular Pain
Volume 14: 1–16
© The Author(s) 2018
Article reuse guidelines:
sagepub.com/journals-permissions
DOI: 10.1177/1744806918814345
journals.sagepub.com/home/mpx
SAGE

Analgesic effects of FAAH inhibitor in the insular cortex of nerve-injured rats

Min Jee Kim[1], Motomasa Tanioka[1], Sun Woo Um[1], Seong-Karp Hong[2], and Bae Hwan Lee[1]

Abstract

The insular cortex is an important region of brain involved in the processing of pain and emotion. Recent studies indicate that lesions in the insular cortex induce pain asymbolia and reverse neuropathic pain. Endogenous cannabinoids (endocannabinoids), which have been shown to attenuate pain, are simultaneously degraded by fatty acid amide hydrolase (FAAH) that halts the mechanisms of action. Selective inhibitor URB597 suppresses FAAH activity by conserving endocannabinoids, which reduces pain. The present study examined the analgesic effects of URB597 treatment in the insular cortex of an animal model of neuropathic pain. Under pentobarbital anesthesia, male Sprague–Dawley rats were subjected to nerve injury and cannula implantation. On postoperative day 14, rodents received microinjection of URB597 into the insular cortex. In order to verify the analgesic mechanisms of URB597, cannabinoid 1 receptor (CB1R) antagonist AM251, peroxisome proliferator-activated receptor alpha (PPAR alpha) antagonist GW6471, and transient receptor potential vanilloid 1 (TRPV1) antagonist Iodoresiniferatoxin (I-RTX) were microinjected 15 min prior to URB597 injection. Changes in mechanical allodynia were measured using the von-Frey test. Expressions of CB1R, N-acyl phosphatidylethanolamine phospholipase D (NAPE-PLD), and TRPV1 significantly increased in the neuropathic pain group compared to the sham-operated control group. Mechanical threshold and expression of NAPE-PLD significantly increased in groups treated with 2 nM and 4 nM URB597 compared with the vehicle-injected group. Blockages of CB1R and PPAR alpha diminished the analgesic effects of URB597. Inhibition of TRPV1 did not effectively reduce the effects of URB597 but attenuated expression of NAPE-PLD compared with the URB597-injected group. In addition, optical imaging demonstrated that neuronal activity of the insular cortex was reduced following URB597 treatment. Our results suggest that microinjection of FAAH inhibitor into the insular cortex causes analgesic effects by decreasing neural excitability and increasing signals related to the endogenous cannabinoid pathway in the insular cortex.

Keywords

Neuropathic pain, insular cortex, fatty acid amide hydrolase inhibitor, URB597, cannabinoid 1 receptor, transient receptor potential vanilloid 1, N-acyl phosphatidylethanolamine phospholipase D

Date Received: 26 April 2018; revised: 10 August 2018; accepted: 30 September 2018

Introduction

Chronic pain results from conditions that compromise or incorporate nerve injury, including spinal lesion, diabetes, and other disorders.[1,2] Long-lasting pain interferes with an individual's social activities and impairs quality of life.[3] Previously, despite their lack of efficacy and potential for unexpected side effects, anodynics such as anti-inflammatories, anticonvulsants, and opioids were used to treat neuropathic pain (NP).[4] However, these therapies are frequently reported to be unsatisfactory or inefficient.[1] Therefore, better therapeutic targets for NP are needed. NP therapy may be improved by identifying and studying

[1]Department of Physiology and Brain Korea 21 PLUS Project for Medical Science, Yonsei University College of Medicine, Seoul, Republic of Korea
[2]Division of Bio and Health Sciences, Mokwon University, Daejeon, Republic of Korea

Corresponding Author:
Bae Hwan Lee, Department of Physiology, Yonsei University College of Medicine, 50-1 Yonsei-ro, Seodaemun-gu, Seoul 03722, Republic of Korea.
Email: bhlee@yuhs.ac

Creative Commons Non Commercial CC BY-NC: This article is distributed under the terms of the Creative Commons Attribution-NonCommercial 4.0 License (http://www.creativecommons.org/licenses/by-nc/4.0/) which permits non-commercial use, reproduction and distribution of the work without further permission provided the original work is attributed as specified on the SAGE and Open Access pages (https://us.sagepub.com/en-us/nam/open-access-at-sage).

efficacious drugs and by targeting specific brain regions that modulate pain signals.

The insular cortex (IC) is an important region of brain associated with the processing of painful stimuli and emotion.[5] The pain matrix, including the IC, is activated by noxious electrical and chemical stimulation, and acute and chronic pain stimulation, as demonstrated by functional magnetic resonance imaging.[6–8] Moreover, lesions of the IC diminish NP-related behaviors in animal models of NP.[9–12]

Among the prospective treatments for NP, cannabinoids are receiving significant attention. Cannabinoids have been recognized for centuries as a potentially useful treatment of diverse illnesses and for their therapeutic effects, including analgesia.[13] However, unfavorable side effects, such as euphoria and hyperphasia, have been observed in mammals treated with plant-derived cannabinoids.[14] These physiological actions are produced via the endogenous cannabinoid neurotransmission system,[15] mainly composed of two G-protein-coupled receptors: cannabinoid 1 receptor (CB1R)[16] and cannabinoid 2 receptor (CB2R).[17] The CB1R, which mediates cannabinoid-induced analgesic effects,[18] is highly expressed in the central and peripheral neurons which mediate excitatory and inhibitory transmitters, including acetylcholine, noradrenaline, and glutamate.[19,20] The CB1R is also found in pain pathways at the central terminals of primary afferent neurons in the brain and spinal cord.[18] Activation of CB1R in the brain inhibits the release of the excitatory neurotransmitter glutamate onto gamma-aminobutyric acid-ergic (GABAergic) neurons.[20] In contrast, the CB2Rs are highly expressed in the immune system and peripheral tissues[17] and is also expressed by neurons in the brain.[21,22] When activated, CB2Rs modulate cytokine release and immune cell migration.[23] However, the role of neuronal CB2R has not yet been established.[14,19]

In mammals, the major endogenous agonists for CB1R and CB2R are N-arachidonoylethanolamine (AEA, anandamide), palmitoylethanolamide (PEA), oleoylethanolamine (OEA), and 2-arachidonoylglycerol (2-AG). These are synthesized "on demand" by postsynaptic neurons and released in retrograde across the synapse via the endocannabinoid membrane transporter to activate CB1R, peroxisome proliferator-activated receptor alpha (PPAR alpha), and CB2R located on the presynaptic neurons.[24–27] Endocannabinoids, AEA and 2-AG, are degraded immediately by intracellular enzymes; AEA is degraded by fatty acid amide hydrolase (FAAH) and 2-AG is degraded by monoacylglycerol lipase.[28,29] The binding affinity of AEA with CB1R is 24-fold less potent than 2-AG.[30] In addition, in rat brain neurons and mouse astrocytes, synthesis of AEA forms N-acyl phosphatidylethanolamine phospholipase D (NAPE-PLD) enzyme which is produced in a Ca^{2+}-dependent manner.[31]

Elevation of endocannabinoids causes robust antinociception in NP models.[32,33] Systemic or intrathecal administration of FAAH inhibitors has shown significant antinociceptive effects in preclinical models of peripheral NP.[34] In particular, the selective FAAH inhibitor URB597 is reported to induce anodynia in several pain models, including heat stimulation, inflammation, and nerve injury-induced pain.[35,36] A previous study reported that FAAH inhibitors significantly increase AEA levels in the brain and mainly induce CB1R-mediated anti-nociception. Therefore, protecting AEA from degradation may produce anti-nociception.[37]

Although anti-nociception through FAAH inhibitors has been observed in various pain models (including NP and inflammatory pain), the role of the FAAH signaling pathway in the IC is unknown. The current study was conducted to determine the effects of inhibiting FAAH in the IC in neuropathic rats.

Materials and methods

Experimental animals

Male Sprague–Dawley rats (180–220 g, Koatec, Pyeongtaek, Korea) were housed in groups of three per cage with 12-h light/dark cycles with food and water provided ad libitum. All experimental procedures and surgeries were performed during the light cycle. Animals were habituated for at least a week before behavioral tests and surgery. All experimental protocols in this study complied with the National Institutes of Health guidelines and approved by the Institutional Animal Care and Use Committee of Yonsei University Health System.

Cannula implantation and NP model

For cannula implantation, rats were fully anesthetized with pentobarbital sodium (50 mg/kg, intraperitoneal (i.p.)) and placed in a stereotaxic frame. The skull was exposed and a 28-gauge guide cannula was implanted in the IC (Bregma: +1.0 mm, Lateral: 4.7 mm, and Ventral: 5.8 mm). Coordinates for the rostral agranular insular cortex (RAIC) were selected according to the rat brain atlas of Paxinos and Watson[38] and Han et al.[39] Each implanted cannula was anchored with three stainless-steel screws and dental acrylic cement. Each guide cannula was capped by a stainless-steel dummy cannula.

NP surgery was performed after cannula implantation. For the NP model (NP group), rats underwent ligation and transection of the sciatic nerve branches under anesthesia with sodium pentobarbital

(50 mg/kg). Briefly, the left sciatic nerve was exposed at the mid-thigh level and carefully removed from the surrounding connective tissue. The three major divisions of the sciatic nerve (tibial, sural, and common peroneal nerves) were separated. Complete ligation and tight transection of the tibial and sural nerves with 4–0 silk sutures were performed, leaving the common peroneal nerve intact.[40] Complete hemostasis was confirmed and then the muscle and skin were closed with silk sutures. For the sham-operated animals (sham group), the left sciatic nerve was exposed, but the nerve branches were left intact without injury. After surgical procedures, the animals were injected with gentamycin to prevent postoperative infection.

Behavioral test for mechanical allodynia

To assess mechanical allodynia, paw withdrawal threshold was measured using an electronic von Frey filament (UGO Basile, Varese, Italy) before nerve injury and on postoperative days (PODs) 1, 4, 7, and 14. Each rat was placed in an acrylic cage ($8 \times 10 \times 20$ cm) with a wire mesh base and allowed to explore for 15 min for experimental familiarization. The electronic von Frey filament was perpendicularly pressed against the sensitive area of the left hind paw. The mechanical threshold was recorded upon the animal flinching from the touch of the von Frey filament. The procedure was conducted seven times per rat.

Drug microinjection into the IC and analgesia test

Animals were divided into groups of seven by their given drugs. They were gently restrained during microinjection. The dummy cannula was removed and a stainless-steel injection cannula connected by polyethylene tubing (PE10) to a Hamilton syringe was inserted via the guide cannula. For behavioral test, rats received bilateral intra-IC microinjections (1 μl/min per side) of vehicle or URB597 (1, 2, and 4 nM, 10046, Cayman Chemical, Ann Arbor, MI, USA). In order to verify the analgesic mechanisms of URB597, different groups of rats received CB1R antagonist AM251 (2 nM, 183232–66-8, Cayman Chemical) (AM251 + URB597 group), PPAR alpha antagonist GW6471 (1 nM, 880635–03-0, Sigma-Aldrich, St. Louis, MO, USA) (GW6471 + URB597 group), and transient receptor potential vanilloid 1 (TRPV1) antagonist I-RTX (1 nM, 1362, Tocris, Bristol, UK) (I-RTX + URB597 group). The selected antagonists were injected 15 min prior to URB597 (4 nM) injection. Veh+Veh and Veh+URB597 groups received vehicle before vehicle or URB597 injection for comparison. Drugs were dissolved in 10% Cremophor EL, 10% dimethyl sulfoxide, 80% saline. Previously, 8 nM of URB597 was tested for its anti-nociceptive effect but was excluded from our presented data due to the similarity of effect compared to 4 nM of URB597 (data not shown). After microinjection, the injection cannula remained in situ for 1 min. The behavioral test was performed pre-microinjection and at 30 min, 1, 2, 4, 8, 12, and 24 h post-microinjection.

Optical imaging

Optical imaging was performed as described in a previous article[39] with slight modification. Male Sprague–Dawley rats (250–300 g; n = 6/group) were fully anesthetized with urethane (1.25 g/kg, i.p.) on POD14 and administered atropine (5 mg/kg, i.p.) to suppress mucus secretion and dexamethasone sulfate (1 mg/kg, i.p.) to reduce swelling of the cortex. Each rat was placed on its sides in a custom-made stereotaxic frame to allow access to the IC located in the anterolateral aspect of the brain. Endotracheal intubation was performed to minimize respiratory movement during the procedure. Craniectomy was conducted and the overlying temporalis muscle, zygomatic arch, and the dura mater was resected to expose the cortex. The cortex was stained using a voltage-sensitive dye (di-2-ANEPEQ, 50 mg/mL in saline; Molecular Probes, Eugene, OR, USA) for 1 h and carefully rinsed with normal saline. Optical imaging was performed directly on the exposed cortex for 30 min before and after the application of vehicle or 4 nM URB597. Dye fluorescence was detected using a high-resolution charge-coupled device camera (Brainvision Inc., Tokyo, Japan) equipped with a dichroic mirror with a 510–550 nm excitation filter and 590 nm absorption filter. A tungsten halogen lamp (150 W) was used for fluorescence excitation. The imaging area was $6.4 \times 4.8\,mm^2$ and consisted of 184×124 pixels.

A pair of stainless-steel electrodes was implanted into the left hind paw where the electronic von Frey filament was applied during behavioral testing. The receptive field was stimulated with a square pulse (width: 0.1 ms, interstimulus interval: 5 s, intensity: 5.0 mA) using a stimulus isolation unit (World Precision Instruments, Sarasota, FL, USA). Fluorescent intensity was detected during each trial for approximately 940 ms under an optical microscope (Leica Microsystems Ltd., Heerbrugg, Switzerland) equipped with a 1× objective and a 1× projection lens. Optical signals were acquired at a rate of 3.7 ms/frame and averaged 30 times by an optical imaging recording system (MiCAM02; Brainvision Inc.). Optical imaging acquisition was triggered by electrocardiogram signals using the stimulus/non-stimulus subtraction method. The amplitudes and excitatory areas of optical signals were measured using a spatial filter (9×9 pixels) to reduce artifacts caused by

vibrations or brain movement. Fractional changes in optical signals (optical intensity) and areas of activation were quantified using captured images. Changes in optical intensity in the IC were calculated as the percentage of fractional change in the intensity of fluorescence ($\Delta F/F \times 100$). Activated areas were analyzed using the activated pixel number of the region of interest (ROI)/total pixel number of the ROI $\times$ 100 (previously described[39]). Data were analyzed using BV Analyzer software (Brainvision Inc.).

Immunohistochemistry

Immunohistochemistry was conducted to verify the target gene of interest using the URB597-injected brains and their vehicle controls. Under urethane anesthesia, each rat was transcardially perfused with normal saline (0.9% NaCl) followed by 4% paraformaldehyde in 0.1 M sodium phosphate buffer (PB, pH 7.4). The brains were removed and immersed in 4% paraformaldehyde in 0.1 M PB for 24 h at 4°C for post-fixation. The brains were kept in 30% sucrose in phosphate-buffered saline (PBS) at 4°C for cryoprotection and frozen in cryostat embedding medium at −70°C (frozen section compound, Leica, Wetzlar, Germany). For immunostaining, each brain was cryosectioned to 20 μm sections on a cryostat (HM 525, Thermo Scientific, Waltham, MA, USA). Slices were washed three times with PBS then incubated in 3% methanol (MeOH).

Sectioned slides were incubated in 4% bovine serum albumin (BSA; Thermo Scientific) in PBS for 1 h at room temperature. Then, they were incubated with rabbit polyclonal anti-CB1R antibody (1:200, ab23703, Abcam, Cambridge, UK) or anti-c-Fos antibody (1:200, AB1584, EMD Millipore, Seattle, WA) diluted in 1% BSA with PBS at 4°C overnight. The following day, the slices were washed three times for 5 min with Tris-buffered saline (TBS) with 1% Tween-20. Then, the slices were incubated in biotinylated anti-rabbit secondary antibody (1:200, BA-1000, Vector Laboratories, Burlingame, CA, USA) or anti-sheep secondary antibody (1:200, BA-6000, Vector Laboratories) for 2 h at room temperature. Slides were then rinsed and incubated with avidin-biotinylated horseradish peroxidase (HRP) complex (1:50, Vector Laboratories) in 0.3% PBS for 1 h. Slides were washed three times for 10 min, and CB1R was visualized by incubating for 5 min in a solution containing 3,3′–diaminobenzidine tetrahydrochloride (DAB) and peroxidase substrate (0.1% of DAB, 0.1% ammonium nickel sulfate, and 0.01% H_2O_2, DAB substrate kit, SK-4100, Vector Laboratories). The slides were washed to stop the DAB reaction, dehydrated in ascending ethanol solutions, and cleared in xylene. All slides were cover slipped using Permount (Fisher Scientific, Waltham, MA, USA).

The distribution of CB1Rs in the IC was determined using Paxinos and Watson's Atlas of the Rat Brain for identification of stereotaxic coordinates.[38] Sections were evaluated with a binocular microscope, and images were captured using a digital camera (Olympus Inc., Melville, NY, USA.). All CB1R images were quantified from light-field microscopy (40× objective, Olympus BX40, Olympus, Tokyo, Japan) with Image J. The number of CB1Rs counted from four sections was averaged for each animal.

Western blot

Animals were deeply anesthetized with isoflurane and decapitated for insular cortices collection. Ipsilateral and contralateral insular cortices were isolated and brain regions were transferred into liquid nitrogen. For protein extraction, isolated tissue was homogenized in lysis buffer (17081, iNtRON Biotechnology Inc., Seongnam, Korea). Homogenate was centrifuged at 22,250 g for 10 min at 4°C, and the supernatant layer was separated from the pellet. The total protein of lysates was assessed with a spectrophotometer (ND-1000, NanoDrop Technologies Inc., Wilmington, DE), and 15 μg of protein for each sample was separated by 10% sodium dodecyl sulfate-polyacrylamide gel electrophoresis. Proteins were transferred onto polyvinylidene difluoride membranes (GE Healthcare, Buckinghamshire, UK). Membranes were blocked in 4% skim milk in TBS with Tween-20 (TBS-T) for 1 h at room temperature and incubated overnight at 4°C with rabbit polyclonal primary antibody to FAAH (1:200, 101600, Cayman Chemicals), NAPE-PLD (1:200, 10305, Cayman Chemicals), CB1R(1:200, 101500, Cayman Chemicals), TRPV1 (1:200, AB5889, EMD Millipore), or glyceraldehyde 3-phosphate dehydrogenase (GAPDH) (1:10,000, FL-335, Santa Cruz Biotechnology, Dallas, TX, USA). The following day, blots were washed in TBS-T buffer and incubated with HRP-conjugated polyclonal anti-rabbit IgG (1:5000, ab6721, Abcam, Cambridge, UK). Immunoreactivity was visualized using a chemiluminescent substrate (ECL Prime Western blotting detection reagent, GE Healthcare) and processed with a local allocation system (ImageQuant LAS 4000 Mini, GE Healthcare). Protein levels were normalized with respect to the signals obtained with the anti-GAPDH antibody.

Quantitative real-time polymerase chain reaction

Approximately 30 mg of frozen tissue was homogenized in 1 ml of RiboEX solution (Geneall Biotechnology, Seoul, Korea) according to the manufacturer's instructions. Purity and concentration of total RNA were measured with a spectrophotometer (ND-1000, NanoDrop

Technologies Inc.,) at 260 nm (A_{260}) and 280 nm (A_{280}). Reverse transcription reactions of total RNA were performed using the SYBR® PrimeScript™ miRNA RT-polymerase chain reaction (PCR) Kit (TaKaRa) with oligodT primer SuperScript III RT (TaKaRa) under the following conditions: 60°C for 60 min followed by 85°C for 5 s, according to the manufacturer's protocol.

Quantitative PCR was performed using a CFX96 detection system (CFX96; Bio-Rad, USA). SYBR® Premix Ex Taq™ II (TaKaRa, Dalian, China) was used to measure relative gene expression in cDNA samples from the sham-operated, NP, and URB597-treated groups. The PCR mixture contained 10 µl of SYBR® Premix Ex Taq™ II, 0.4 µl of ROX solution, 1 µl of specific primer, 1 µl of RT reaction solution, and 5.6 µl of dH_2O. Quantitative PCR was performed with primers specific for NAPE-PLD, CB1R, CB2R, FAAH, and TRPV1 under the following conditions: 95°C for 30 min, followed by 40 cycles at 95°C for 5 s, and 60°C for 20 s. After PCR, amplification and melting curves were checked and the mRNA concentration was calculated (Bio-Rad CFX Manager, Hercules, CA, USA) and represented as mean $2^{-\Delta\Delta CT} \pm$ standard deviation. Average CT values were normalized for GAPDH mRNA from the same cDNA preparations. Results presented are expressed as fold increases over control values. The following primers were used: FAAH (Reverse: 5′-TCCACTGGGCAATCACAGAC-3′, Forward: 5′-CAGTATGCGTCCTCGGTCAG-3′); NAPE-PLD (Reverse: 5′-TCAAGCTCCTCTTTGG AACCC-3′, Forward: 5′-CATGGCCAACGTGGA AGAAC-3′); CB1R: (Reverse: 5′-GGAGGGAACC CTCAGCCAT-3′, Forward: 5′-GGAGAACTTACT GTGAACAGGC-3′); and GAPDH (Reverse: 5′-GGTGGTGAAGACGCCAGTAG-3′, Forward: 5′-CA CCATCTTCCAGGAGCGAG-3′).

Statistical analysis

Data were presented as means ± standard error of the mean. Statistical significance was determined using the paired or unpaired *t* tests between groups, one-way analysis of variance (ANOVA) with Dunnett's or Bonferroni's post hoc analysis, and two-way ANOVA with Bonferroni's post hoc analysis. In all cases, P-values less than 0.05 were considered significant.

Results

Peripheral nerve injury leads to the development of mechanical allodynia

Time-dependent behavioral changes were examined in neuropathic rats by measuring mechanical threshold at POD1, 4, 7, and 14 after NP surgery. The mechanical threshold of the NP group was significantly lower than that of the sham-operated group on POD1 ($P < 0.05$), POD4 ($P < 0.001$), POD7 ($P < 0.001$), and POD14 ($P < 0.001$) (Figure 1; $n = 7$, two-way repeated measured ANOVA followed by Bonferroni's multiple comparison).

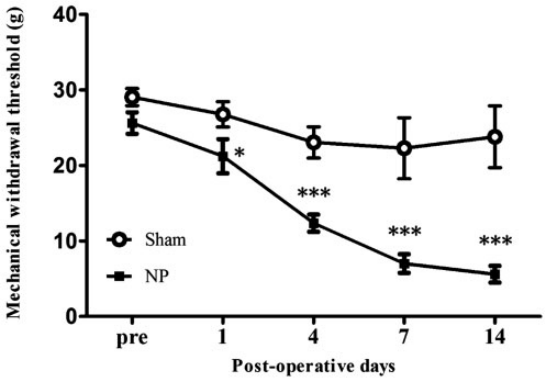

Figure 1. Development of mechanical allodynia in neuropathic rat. After nerve injury, animals developed significant mechanical allodynia on POD1, POD4, POD7, and POD14 compared with the sham-operated group. Data are presented as means ± standard error of the mean. *$P < 0.05$; ***$P < 0.001$. Two-way repeated analysis of variance followed by Bonferroni's post hoc multiple comparison test. NP: neuropathic pain group.

NP activates FAAH signaling-related factors in the IC

To determine whether nerve injury can cause FAAH-related molecular changes, mRNA expression levels of FAAH signaling-related proteins CB1R, NAPE-PLD, FAAH, and TRPV1 were measured in the IC POD14 after nerve injury. The results indicate that on POD14, mRNA levels were upregulated for CB1R, NAPE-PLD and TRPV1 in the NP group ($n = 6$) compared with mRNA levels of the aforementioned proteins in the sham-operated group (Figure 2; $n = 6$ each group, $P < 0.05$, two-way repeated measure ANOVA followed by Bonferroni's multiple comparison). However, there were no differences in FAAH levels (Figure 2(c), $P > 0.05$). These results suggest that the FAAH signaling pathway in the IC is strongly related to NP.

Expression of FAAH signaling-related proteins in the IC after nerve injury

To further investigate protein alterations related to FAAH signaling in the IC resulting from NP, protein levels of CB1R, NAPE-PLD, FAAH, and TRPV1 in the IC were measured POD14 after nerve injury. NP caused by peripheral nerve injury resulted in significantly elevated levels of CB1R, NAPE-PLD, and TRPV1 (Figure 3 (a), (b), and (d); $n = 7$, each group, $P < 0.05$, unpaired *t*

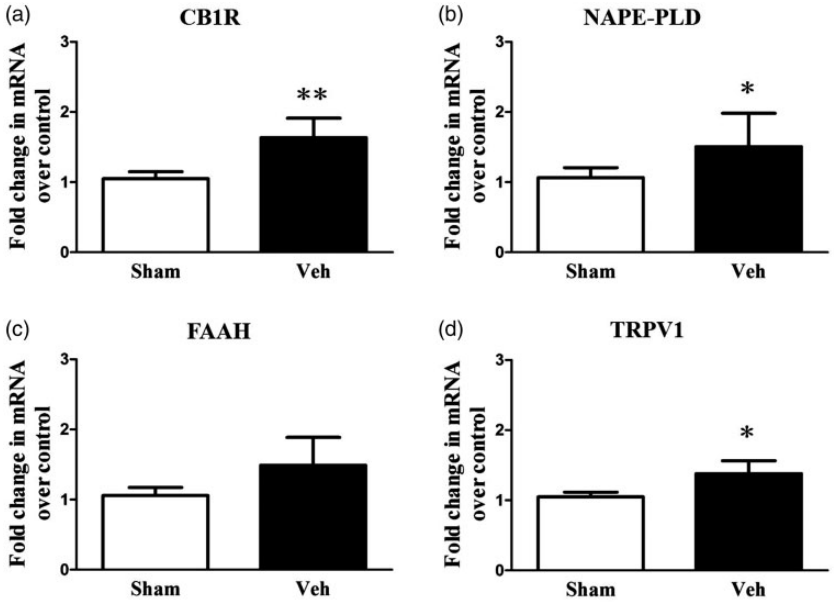

Figure 2. mRNA expression of CB1R, NAPE-PLD, and TRPV1 increases in the insular cortex (IC) of neuropathic rats. Quantitative reverse transcription polymerase chain reaction (RT-PCR) was used to measure CB1R (a), NAPE-PLD (b), FAAH (c), and TRPV1 (d) mRNA in the IC of the neuropathic group (NP, n = 6) and the sham-operated group (sham, n = 6). CB1R, NAPE-PLD, and TRPV1 mRNA levels were significantly up-regulated in the NP group compared with the sham group, but the level of FAAH was not significantly different between NP and sham groups. Results are presented as a fold change normalized to GAPDH expression. Data are presented as mean ± standard error of the mean. Asterisks indicate statistical significance compared with the sham group; *$P < 0.05$; **$P < 0.01$, unpaired *t* test. NP: neuropathic pain; CB1R: cannabinoid receptor 1; NAPE-PLD: N-acyl phosphatidylethanolamine phospholipase D; FAAH: fatty acid amide hydrolase; TRPV1: transient receptor potential vanilloid 1.

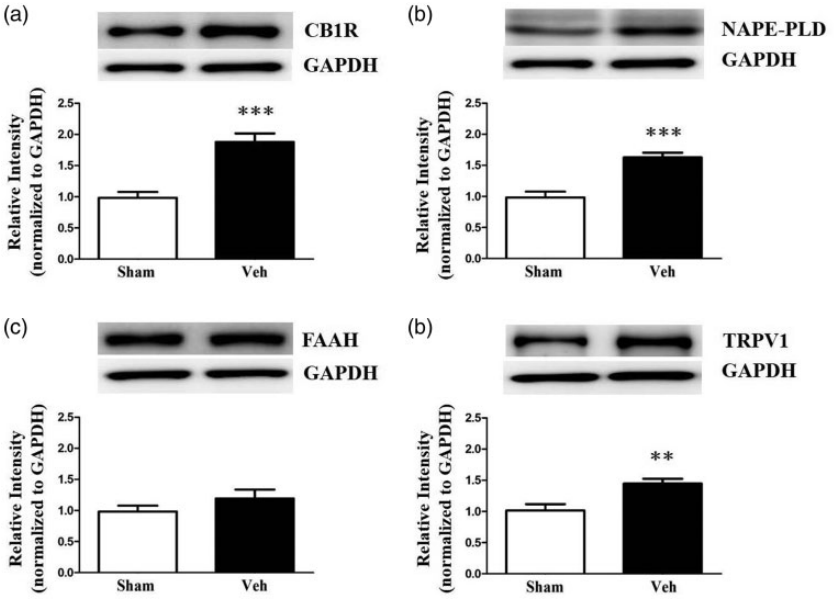

Figure 3. Changes in expression levels of FAAH-related proteins in the insular cortex (IC) of neuropathic rats. Protein expressions of CB1R (a), NAPE-PLD (b), and TRPV1 (d) in the IC were upregulated in the neuropathic group (NP, n = 6) compared with the sham-operated group (sham, n = 6), but the level of FAAH (c) was not significantly different between NP and sham groups. Representative images of Western blot bands are shown with GAPDH as a loading control. Data are presented as mean ± standard error of the mean. Asterisks indicate significance compared with the sham group; **$P < 0.01$; ***$P < 0.001$, unpaired *t* test. NP: neuropathic pain, CB1R: cannabinoid receptor 1; NAPE-PLD: N-acyl phosphatidylethanolamine phospholipase D; FAAH: fatty acid amide hydrolase; TRPV1: transient receptor potential vanilloid 1; GAPDH: glyceraldehyde 3-phosphate dehydrogenase.

test), although there was no change in FAAH levels (Figure 3(c); $n = 7$, $P > 0.05$). Increased CB1R and TRPV1 expression in the IC may contribute to the analgesic efficacy of FAAH activity inhibition in NP rats.

URB597 microinjection into the IC reduces the mechanical threshold

Systemic or intrathecal administration of URB597 has been shown to reduce NP.[41] However, it is unknown if direct administration of URB597 into the IC reduces pain. Here, the effects of URB597 in the IC of a rat model of NP were investigated. Behavioral changes of the dose-dependent effects of URB597 were tested in four groups: 1 nM, 2 nM, 4 nM URB597-microinjected neuropathic groups, and the vehicle-treated NP group. Before microinjection, the mechanical threshold was measured, then microinjections to the IC were conducted for the four treatment groups. Between 0.5 and 2 h after microinjection of the FAAH inhibitor URB597, the mechanical threshold was significantly increased at doses of 2 nM and 4 nM of URB597 (Figure 4(a); $n = 7$ each group, $P < 0.05$, two-way repeated measure ANOVA followed by Bonferroni's multiple comparison) but not at a 1 nM dose or in the vehicle treatment (Figure 4(a); $n = 7$ each group, $P > 0.05$).

The effects of different specific antagonists (AM251, GW6471 or I-RTX) followed by URB597 (4 nM) on mechanical threshold were examined 14 days after nerve injury surgery (Figure 4(b)). The marked inhibitory effect of 4 nM URB597 was attenuated by pretreatment with the selective CB1R antagonist AM251 (Figure 4(b); $n = 7$ each, $P < 0.05$, two-way repeated measure ANOVA followed by Bonferroni's multiple comparison). Antagonists for CB1R and PPAR alpha effectively reduced the analgesic effects of URB597 (Figure 4(b); $n = 7$ each group, $P < 0.05$, two-way repeated measure ANOVA followed by Bonferroni's multiple comparison). However, PPAR antagonist GW6471 did not completely attenuate the pain-relieving effects of URB597 compared to CB1R antagonist AM251. Such results indicate that the analgesic mechanism of URB597 involves CB1R more than PPAR alpha.

Inhibition of FAAH by URB597 reduces IC excitability during NP

In this study, optical signals in the IC increased in nerve-injured rats after peripheral electrical stimulation. Representative optical images were obtained by electrical stimulation (5 mA) of the contralateral hind paw in nerve-injured rats before and after drug treatment (Figure 5). Wave forms represent optical responses at specific time points in each image of the IC. Figure 5 (a) and (b) is representative images before and after treatment with either vehicle or 4 nM URB597.

Peak amplitudes and activated areas of the IC are represented in Figure 5(c) and (d), respectively. The

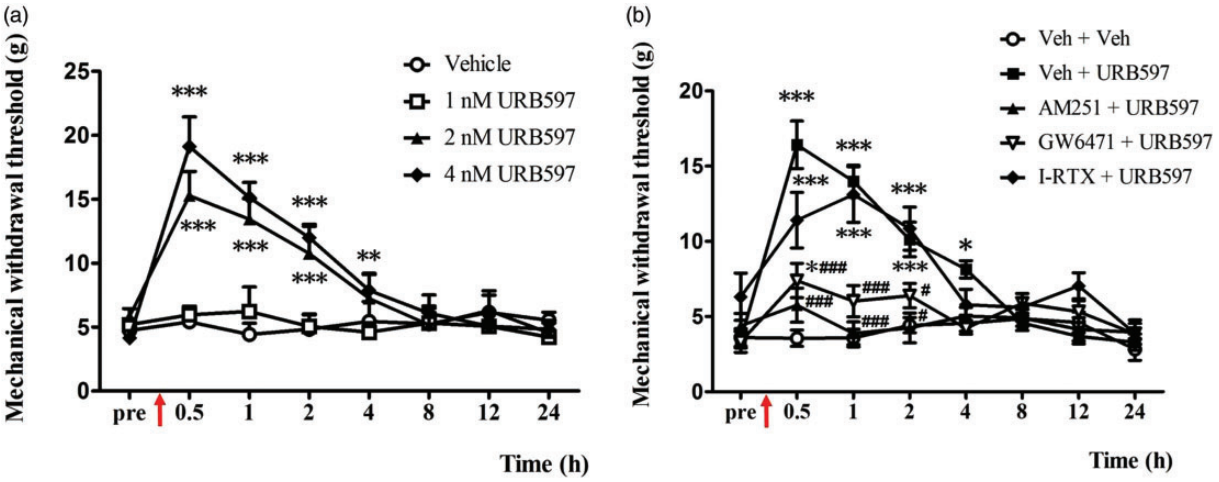

Figure 4. Changes in paw withdrawal thresholds in response to mechanical stimulation after microinjection of vehicle or URB597 with different doses and pretreatment of antagonists (AM251, GW6471, or I-RTX) on POD14. (a) Microinjection of URB597 attenuates mechanical allodynia in a dose-dependent manner. Arrow indicates time point of microinjection. Significant differences in withdrawal threshold between 2 nM or 4 nM URB597 and vehicle-treated groups were observed between 0.5 h and 4 h after microinjection. The changes with the highest significance in withdrawal threshold were observed in the 4 nM URB597-treated group, with significant changes observed between 0.5 h and 4 h after microinjection. (b) Analgesic effects of 4 nM URB597 were significantly blocked by pre-administration of AM251 or GW6471 followed by URB597 injection compared with the Veh + URB597 group which has not been blocked at all. Data are represented as means ± standard error of the mean; $n = 7$ rats/group, $^{*}P < 0.05$; $^{**}P < 0.01$; $^{***}P < 0.001$ vs. sham (a), $^{*}P < 0.05$; $^{***}P < 0.001$ vs. Veh + Veh; $^{\#}P < 0.05$; $^{\#\#}P < 0.01$; $^{\#\#\#}P < 0.001$ vs. Veh + URB597 (b). Two-way repeated measure analysis of variance followed by Bonferroni's post hoc multiple comparison test.

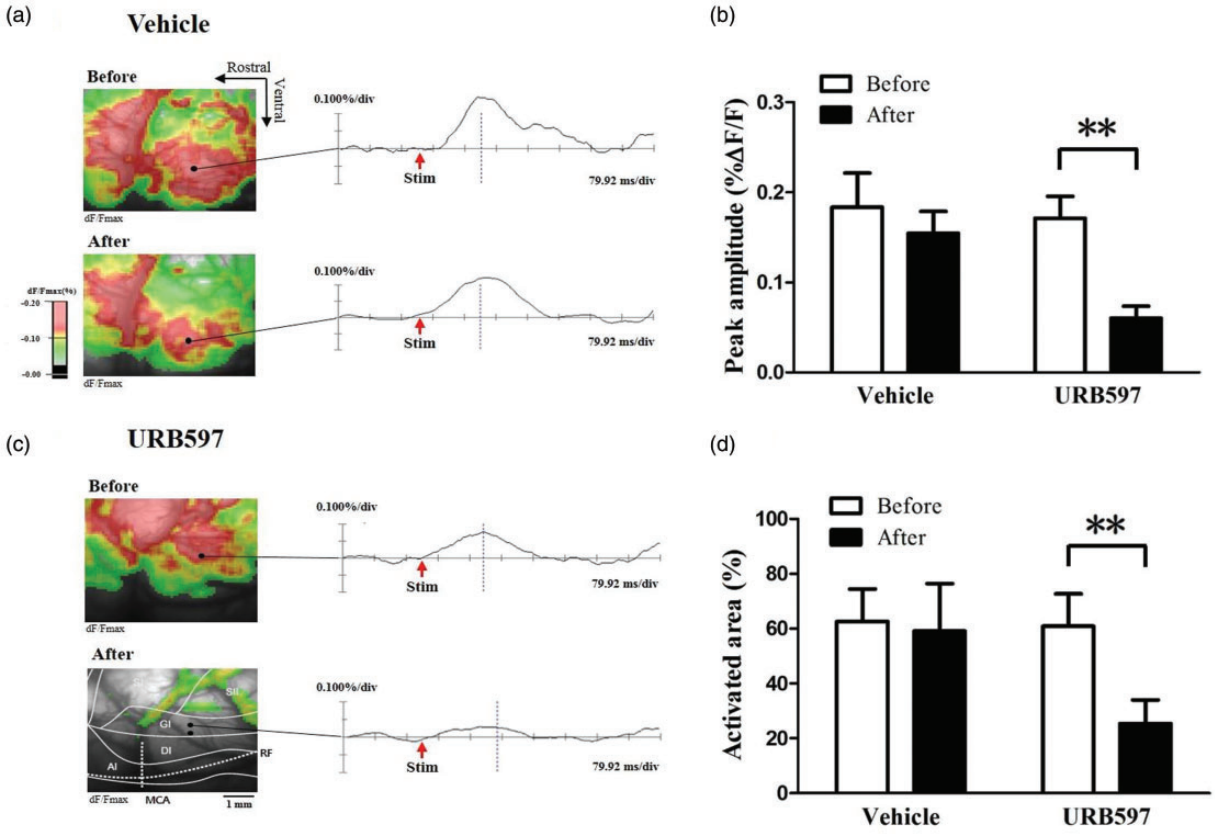

Figure 5. Changes in optical signals from the insular cortex (IC) before and after treatment with 4 nM URB597 or vehicle in nerve-injured rats. (a) Optical images before and after t vehicle treatment in nerve-injured rats. (b) Optical images before and after 4 nM URB597 treatment in a nerve-injured rat with location of the IC. Activated area is color-coded, and the data from optical signals are represented as the percent of change in fluorescent intensity (%ΔF/F). (c) Peak amplitudes before and after treatments with vehicle or URB597 in response to 5.0 mA electrical stimulation of the left hind paw in nerve-injured rats. (d) Activated area before and after vehicle or 4 nM URB597 treatment in response to 5.0 mA electrical stimulation of the left hind paw in nerve-injured groups. Peak amplitudes and activated areas induced by peripheral electrical stimulation after 4 nM URB597 microinjection were significantly lower than those before URB597 treatment. There were no significant changes in peak amplitudes and activated areas before and after vehicle treatment. Data are presented as mean ± standard error of the mean. $^{**}P < 0.01$, paired *t* test.

peak amplitude evoked by 5.0 mA peripheral electrical stimulation of neuropathic rats was reduced after URB597 treatment compared to before treatment (Figure 5(c); $n = 6$, $P < 0.01$, paired *t* test). The activated areas in response to electrical stimulation in neuropathic rats decreased after URB597 treatment compared to before treatment (Figure 5(d); $n = 6$, $P < 0.01$, paired *t* test). However, there were no significant differences in peak amplitudes or activated areas before and after vehicle treatment in the IC of neuropathic rats (Figure 5(c) and (d), $P > 0.05$).

Inhibition of FAAH reduces neuronal activation related to IC pain

To further confirm enhanced cortical activity in response to NP, c-Fos expression in the IC was examined using immunohistochemistry. As shown in Figure 6, the number of cells positive for c-Fos in the IC increased on POD14 compared with the sham-operated groups (Figure 6(a) and (b)). On POD14, the NP rats had a higher number of c-Fos-positive cells than rats receiving 4 nM URB597 injections (Figure 6(a), photomicrographs and Figure 6(b), a graph of c-Fos-positive cells, $n = 6$ each group, $P < 0.05$, unpaired *t* test). These results indicate that neuronal activity of the IC is enhanced in response to NP and is also attenuated by FAAH inhibition.

Nerve injury elevates CB1R in the IC

The IC is important for modulating the sensory components of pain.[42] To elucidate the involvement of the IC in the anti-allodynic effects of URB597, immunohistochemistry was performed 30 min after injection of 4 nM URB597 or vehicle. On POD14, expression of CB1Rs was observed by marked dark staining in the IC of NP rats. The number of CB1R-positive cells

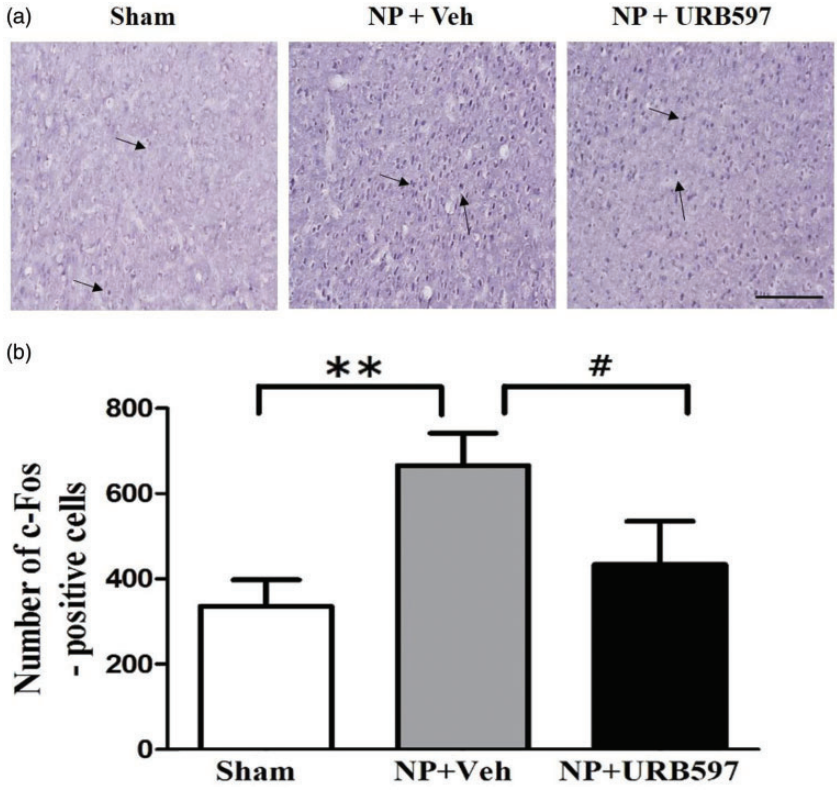

Figure 6. Changes in c-Fos expression after microinjection of URB597 in the insular cortex (IC). (a) Representative photomicrographs of c-Fos-positive cells in the IC. Arrows indicate c-Fos-positive cells on POD14. (b) Number of c-Fos-positive cells in the IC of sham-operated, vehicle-treated neuropathic, and 4 nM URB597-treated neuropathic groups on POD14. c-Fos expression was significantly higher in the vehicle-treated neuropathic group (NP + Veh) than the sham-operated group (sham). After microinjection of 4 nM URB597, the number of c-Fos-positive cells decreased in the IC of NP rats (NP + URB597). Scale bars, 200 μm. Data are presented as means ± standard error of the mean, $^{**}P < 0.01$, vs. sham. $^{\#}P < 0.05$ vs. NP + 4 nM, One-way analysis of variance followed by Bonferroni's post hoc multiple comparison test. NP: neuropathic pain.

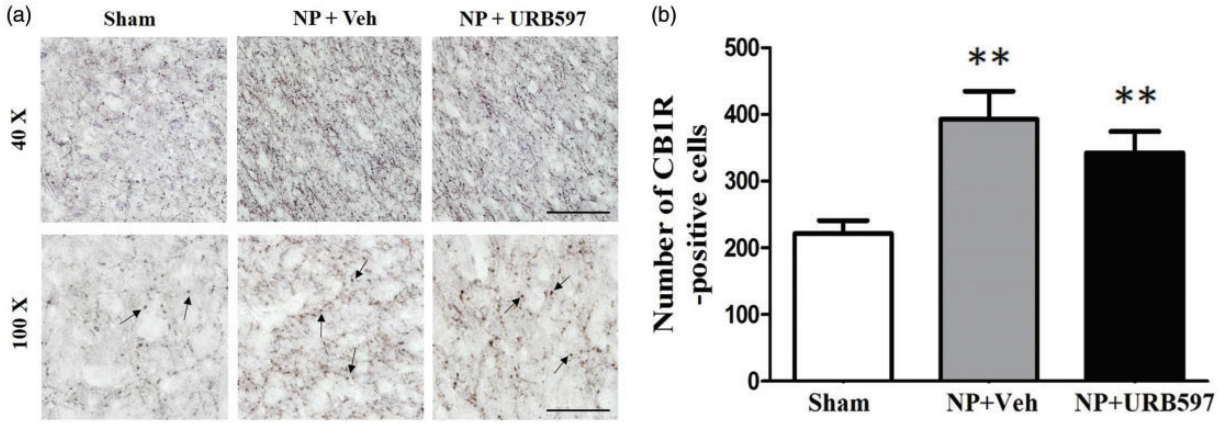

Figure 7. Changes in CB1R in the insular cortex (IC) after microinjection of 4 nM URB597 in neuropathic rats. (a) Representative low (above) and high (below) magnificent photomicrographs of CB1R-positive cells in the IC of sham-operated, vehicle-treated neuropathic, and 4 nM URB597-treated neuropathic groups on POD14. Arrows indicate CB1R-positive cells. (b) Number of CB1R-positive cells in the IC of sham-operated, vehicle-treated neuropathic, and 4 nM URB597-treated neuropathic groups on POD14. Expression of CB1R increased significantly after nerve injury compared with the sham-operated group. Microinjection of 4 nM URB597 did not change CB1R expression in the IC even though it tended to reduce CB1R expression slightly. Scale bars, 100 μm (above), 50 μm (below). Data are presented as means ± standard error of the mean. $^{**}P < 0.01$; $^{***}P < 0.001$ vs. sham, One-way analysis of variance followed by Dunnett's post hoc multiple comparison test. NP: neuropathic pain.

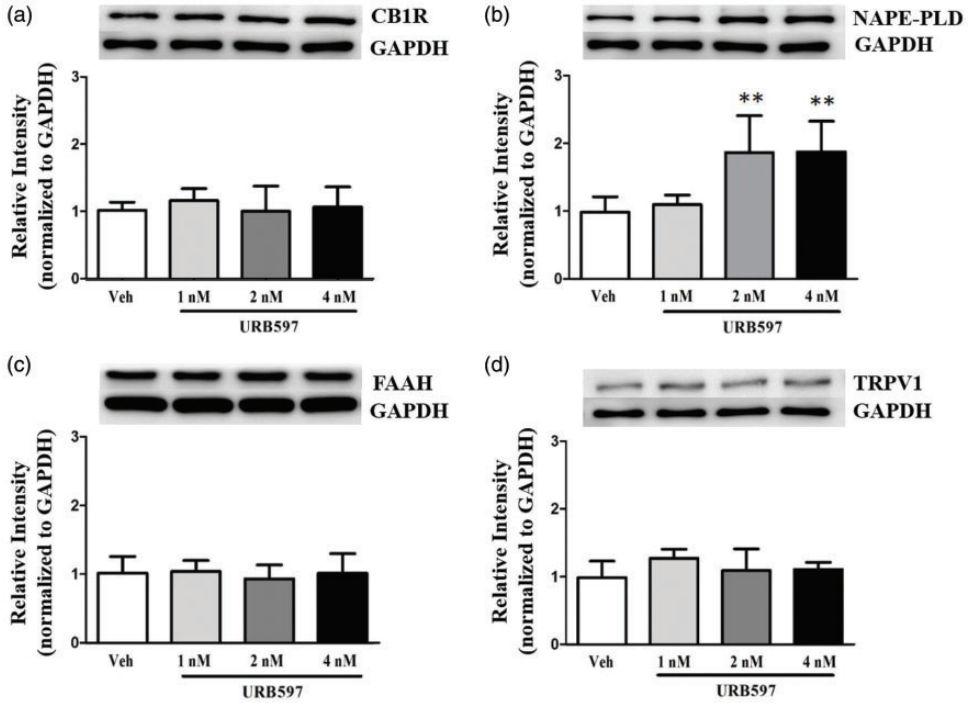

Figure 8. Effects of URB597 on expression of CB1R, NAPE-PLD, FAAH, and TRPV1 in the insular cortex (IC) of neuropathic rats revealed by Western blots. Expression levels of CB1R (a), NAPE-PLD (b), FAAH (c), and TRPV1 (d) were observed after microinjection of URB597. Levels of NAPE-PLD were significantly increased in the 2 nM and 4 nM URB597-treated groups compared with the vehicle-treated group. Levels of CB1R, FAAH, and TRPV1 were similar among groups. Representative images of Western blots are shown with GAPDH as a loading control. Histograms represent the mean ± standard error of the mean of quantified Western blot band intensities ($n = 7$/group). **$P < 0.01$, vs. vehicle-treated group. One-way analysis of variance followed by Dunnett's post hoc multiple comparison test. CB1R: cannabinoid receptor 1; NAPE-PLD: N-acyl phosphatidylethanolamine phospholipase D; FAAH: fatty acid amide hydrolase; TRPV1: transient receptor potential vanilloid 1; GAPDH: glyceraldehyde 3-phosphate dehydrogenase.

counted on POD14 in the nerve-injured group was significantly higher than that of the sham-operated group (Figure 7(a), second lane photomicrographs and Figure 7(b), graph of CB1R-positive cells, $n = 6$ per groups, $P < 0.01$, $P < 0.001$, unpaired t test). However, the expression of CB1R after the 4 nM URB597 treatment was not significantly different for vehicle treatment alone (Figure 7, $n = 6$ each group, $P > 0.05$).

Microinjection of URB597 into the IC increases levels of NAPE-PLD

Western blot analysis was performed to determine the effect of intracranial administration of URB597 on the FAAH signaling pathway, specifically the proteins CB1R, NAPE-PLD, FAAH, and TRPV1, which are activated by the endocannabinoid ligand AEA.[43] One-way ANOVA showed significantly higher NAPE-PLD protein expression in the 2 nM and 4 nM URB597 injection groups than the vehicle-treated group (Figure 8(b), $P < 0.01$). However, protein expression of other FAAH signaling components did not significantly change following URB597 microinjection. Specifically, the levels of CB1R (Figure 8(a), $P > 0.05$), FAAH (Figure 8(c), $P > 0.05$), and TRPV1 (Figure 8(d), $P > 0.05$) did not change in rats receiving different doses of URB597 or vehicle treatment.

mRNA expression of endocannabinoid components

To address whether the changes observed in FAAH signaling-related components after URB597 microinjection into the IC were associated with the nerve-injured state, the gene expressions of CB1R, NAPE-PLD, FAAH, and TRPV1 in the IC were analyzed. Similar to the Western blot results, only the mRNA levels of NAPE-PLD were changed in the 4 nM URB597-treated group (Figure 9(b), $P < 0.001$, one-way repeated measure ANOVA followed by Bonferroni's multiple comparison). There were no other significant changes found in the gene expression of other endocannabinoid-related components CB1R, FAAH, and TRPV1 (Figure 9(a), (c), and (d), $P > 0.05$).

Blockage of TRPV1 attenuates levels of NAPE-PLD increased by FAAH inhibitor

Western blot analysis was conducted to determine if inhibition of CB1R, PPAR alpha, or TRPV1 would

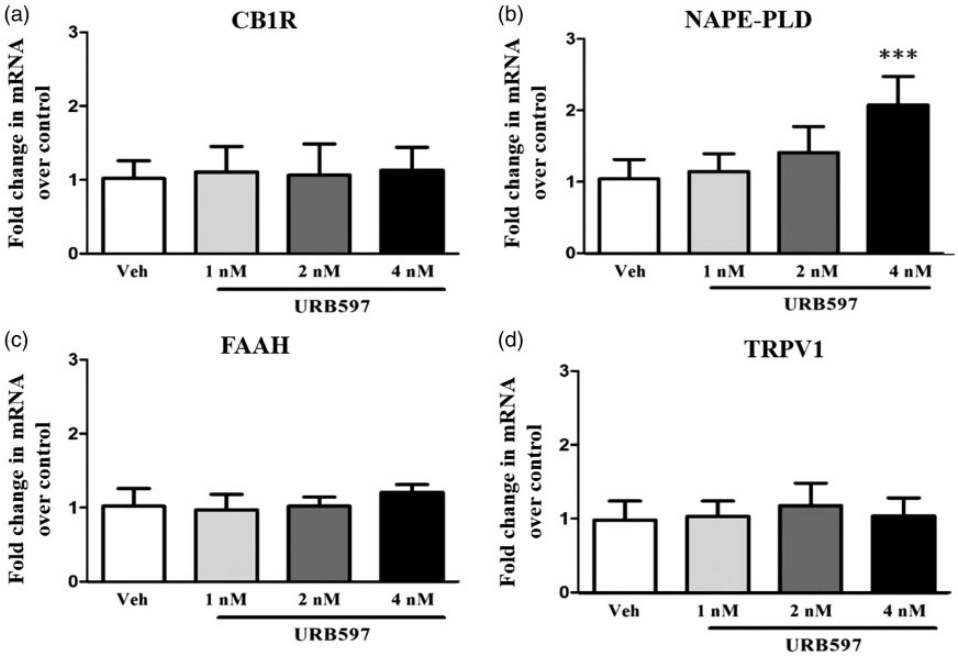

Figure 9. Changes in mRNA levels of FAAH signaling components following URB597 microinjection into the insular cortex (IC) of neuropathic rats. CB1R (a), NAPE-PLD (b), FAAH (c), and TRPV1 (d) gene expression levels in the IC were observed after microinjection of vehicle or URB597 at 1 nM, 2 nM, or 4 nM. Level of NAPE-PLD was significantly increased in the 4 nM URB597-treated group compared with the vehicle-treated group. Levels of CB1R, FAAH, and TRPV1 in all groups did not change dose dependent manner ((a), (c) and (d)). Data are presented as the mean ± standard error of the mean (n = 6/group). Results are presented as fold change normalized to GAPDH expression. ***$P < 0.001$, vs. vehicle-treated group. One-way analysis of variance followed by Dunnett's post hoc multiple comparison test. CB1R: cannabinoid receptor 1; NAPE-PLD: N-acyl phosphatidylethanolamine phospholipase D; FAAH: fatty acid amide hydrolase; TRPV1: transient receptor potential vanilloid 1.

affect the expressions of FAAH-related proteins in the IC of neuropathic rats. Pre-administration of TRPV1 antagonist into the IC reduced NAPE-PLD expression levels elevated by URB597 compared to vehicle-treated group (Figure 10(b), $P < 0.01$, one-way repeated measure ANOVA followed by Bonferroni's multiple comparison). Neither the AM251+URB597 nor GW6471+URB597 groups altered their expression of NAPE-PLD (Figure 10(b), $P > 0.05$). There were no significant differences in expression levels of CB1R (Figure 10(a), $P > 0.05$), FAAH (Figure 10(c), $P > 0.05$), and TRPV1 (Figure 10(d), $P > 0.05$) in AM251+URB597, GW6471+URB597, and I-RTX + URB597 groups compared to Veh+URB597 group.

Discussion

Despite extensive interest, many aspects of the mechanism for NP remain unknown.[44,45] The present study provides integrated behavioral, electrophysiological, and biochemical evidence showing pain modulation via FAAH inhibition in the IC after peripheral nerve injury. Increasing endocannabinoids by blocking FAAH has antinociceptive effects in NP.[46] Consequently, FAAH inhibition may provide a novel strategy for anti-allodynic drugs. There are no reports of FAAH signaling related to modulation of NP in the IC. The selective FAAH inhibitor URB597 was used to inhibit FAAH activity in an animal model of NP. It suppressed NP through the conservation of the endocannabinoid AEA in the IC.[46–48] In addition, the inhibition of CB1R or PPAR alpha reversed the anti-nociceptive effects of URB597. However, the efficacy in attenuating pain was significantly lower by antagonizing PPAR alpha rather than CB1R. These results indicate that CB1R may be more involved in the anti-nociceptive mechanism compared to PPAR alpha, according to the inhibition of these particular receptors in our pain model. Consequently, we may conclude that AEA may be relatively more involved in the pain-relieving process than PEA in the IC. This study is the first to demonstrate the potential anti-allodynic effects of URB597 in the IC and provides evidence to support a pain modulation role for the FAAH signaling pathway in the IC.

Studies have shown that the IC has an important role in the pain modulation process[5,49] and consists of multiple neurotransmitter systems related to pain, including cannabinergic, opioidergic, serotoninergic, and dopaminergic transmissions.[50,51] Moreover, previous studies demonstrated a significant increase in both mRNA and

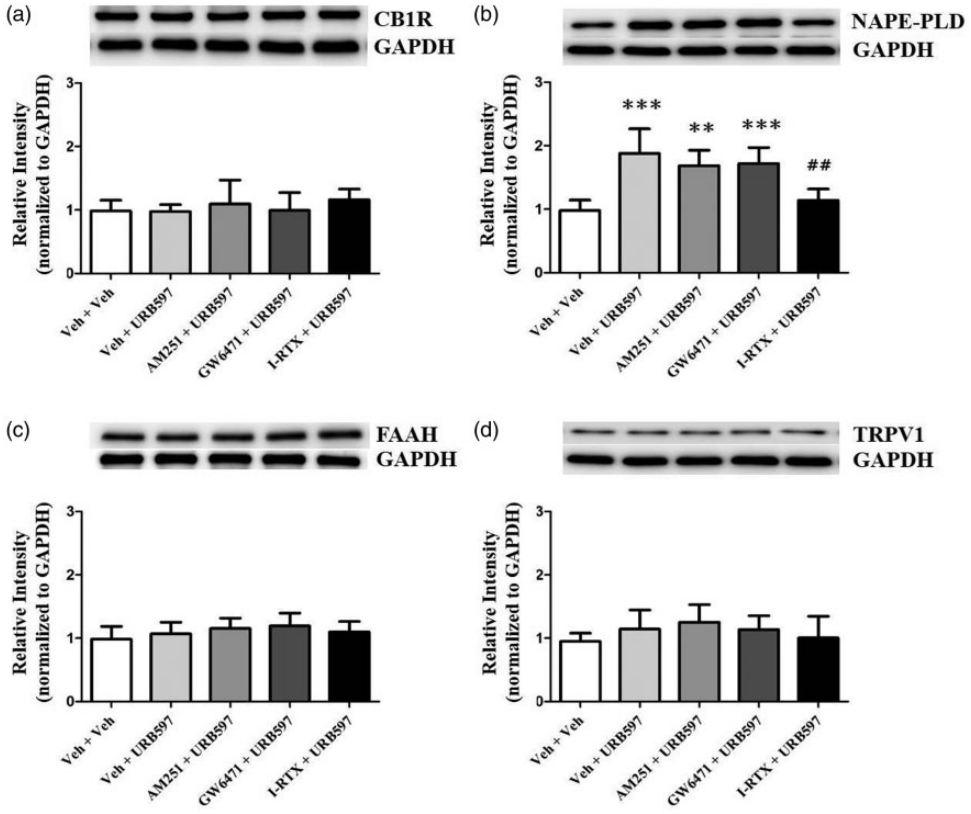

Figure 10. Comparison of the expression of CB1R, NAPE-PLD, FAAH, and TRPV1 in the insular cortex of neuropathic rats after pretreatment of antagonists (AM251, GW6471, or I-RTX) followed by URB597. Expression levels of CB1R (a), NAPE-PLD (b), FAAH (c), and TRPV1 (d) were observed after pre-administration of antagonist (2 nM AM251, 1 nM GW6471, or 1 nM I-RTX) with 4 nM URB597. Expression of NAPE-PLD was significantly increased in the Veh + URB597 groups compared with the Veh + Veh group and decreased in the I-RTX + URB597 group compared to the Veh + URB597 groups. Histograms represent mean ± standard error of the mean of quantified Western blot band intensities (n = 7/group). $^{**}P < 0.01$; $^{***}P < 0.001$, vs. Veh + Veh group. $^{\#\#}P < 0.01$ vs. Veh + URB597. One-way analysis of variance followed by Bonferroni's post hoc multiple comparison test. CB1R: cannabinoid receptor 1; NAPE-PLD: N-acyl phosphatidylethanolamine phospholipase D; FAAH: fatty acid amide hydrolase; TRPV1: transient receptor potential vanilloid 1; GAPDH: glyceraldehyde 3-phosphate dehydrogenase.

protein expression levels of CB1R, TRPV1, and NAPE-PLD in the dorsal root ganglion of neuropathy rats during the development or maintenance of pain.[42,52] Similarly, the results of this study demonstrated a decrease in mechanical threshold after nerve injury on POD14 and an increase in the mRNA and protein expression levels of CB1R, NAPE-PLD, and TRPV1 in the IC of nerve-injured rats. Such robust expression levels provide evidence that NP is modulated through changes in FAAH signaling in the IC.

FAAH inhibitor URB597 reduces the nociceptive response caused by inflammatory and NP via systemic or intrathecal administration[41] and these pain-relieving effects can be blocked by cannabinoid receptor antagonists.[53,54] In this study, changes in the mechanical threshold were observed after direct injection of the FAAH inhibitor into the IC of peripheral nerve-injured rats. In particular, microinjection of URB597 at doses of 2 nM and 4 nM significantly reduced mechanical allodynia on POD14. However, the analgesic effect did not persist for 8 h after injection. These results suggest that URB597 reduces NP by inhibiting the activation of FAAH.

We performed an electrophysiological study to examine neuronal excitation induced by NP and studied the inhibitory effects of URB597 on pain signals. We observed distinct changes in neuronal activation under NP conditions after URB597 treatment in the IC. Our previous studies presented a visualization of neuronal excitation in the IC after peripheral nerve injury.[39,55] To examine changes in excitatory patterns in the IC between the neuropathic group and URB597-treated group, the neuronal signals induced by electrical stimulation of the left hind paw were recorded. We observed that neuronal activity in neuropathic rats increased in the peripheral nerve injury group, and neuronal activity

in the IC was inhibited by URB597 treatment. Moreover, we found that the increases of neuronal activity coincided with elevated c-Fos expression which is an immediate early marker of neuronal activation.[56,57] The expression of c-Fos increased after nerve injury and decreased after URB597 microinjection in the IC. These results indicate that the IC is closely involved in nociception information processing, and URB597 could reduce the response to peripheral nerve injury in the IC.

Previous studies reported increased CB1R mRNA expression in the dorsal root ganglion[42] and spinal cord neurons[58] after nerve injury. In this study, increased expressions of both CB1R mRNA and protein were observed, as well as an increase in CB1R-positive cells in the IC on POD14 after peripheral nerve injury. The increase in CB1R expressions results in augmented potency or efficacy of the up-regulated levels of AEA.[59] It is also likely that increased CB1R expression contributes to the effectiveness of AEA which provides relief from painful neuropathy symptoms after inhibition of FAAH. Moreover, NP can induce synaptic plasticity and long-term potentiation (LTP) involved in the glutamatergic systems of the IC.[60,61] In this sense, glutamate and GABArelease can be modulated by AEA and CB1R in the presynaptic terminals, and the activation of CB1R by increased AEA through the inhibition of FAAH may decrease synaptic transmission to prevent LTP.[60] Thus, URB597 may produce analgesic effects by activating CB1R and consequently inhibiting LTP.[62,63]

Several studies have shown that FAAH inhibition attenuates mechanical allodynia and thermal hyperalgesia in NP models.[36,64,65] Also, NAPE-PLD which is synthesized in tissue elevates AEA levels.[66,67] This activity may be interpreted as an endogenous defense mechanism against pain. Accordingly, we observed that microinjection of 2 nM and 4 nM URB597 increased NAPE-PLD expression in the IC of nerve-injured rats. The analgesic effect of AEA produced by NAPE-PLD in neuropathic conditions is difficult to observe because AEA is immediately degraded by FAAH.[46] Although FAAH is the dominant enzyme that metabolizes AEA in the brain,[68] it is unknown how the metabolic pathways of FAAH signaling in the IC contribute to NP. Besides its role in activating cannabinoid receptors,[22,69] AEA also activates TRPV1 receptors, which may produce an analgesic effect.[58] Elevating AEA levels by FAAH inhibition could cause simultaneous activation of conflicting mechanisms of cannabinoid receptors and TRPV1 to suppress or induce pain, respectively.

Here, we provide evidence that inhibition of FAAH may contribute to analgesic effects induced by increasing the expression of NAPE-PLD. As mentioned, AEA which is synthesized by NAPE-PLD activates CB1R, CB2R, and TRPV1. In this study, Western blot and qPCR analysis confirmed that TRPV1 is present in the IC. According to a previous study, AEA activates CB1R after URB597 injection and may increase levels of NAPE-PLD protein or mRNA expression via TRPV1 activity.[43] The concentration of calcium ion in postsynaptic neurons is probably increased by the pain signal-induced release of glutamate in the presynaptic neurons, thereby synthesizing more NAPE-PLD that produces AEA.[38,58] Then, AEA may be released to the synaptic cleft from postsynaptic neurons via a membrane transporter, thus activating the CB1R in the presynaptic neurons.[42,66] Consequently, the influx of calcium ions in the presynaptic neurons is blocked by CB1R activation, which prevents the release of glutamate. Because NAPE-PLD synthesis is dependent on the concentration of calcium ion,[14] the expression of NAPE-PLD may decrease due to a glutamate release that is inhibited by the reduction of pain. However, in the current study, we noted elevated NAPE-PLD expression, which may indicate that AEA activates TRPV1 channels and subsequently increases calcium ion concentration. Although the activity of TRPV1 sustains and induces pain,[70] the calcium ion influx mediated by this channel in the cannabinoid signaling pathway may prompt NAPE-PLD synthesis, which leads to the production of AEA and the reduction of pain.[71] In order to confirm our hypothesis, reduced levels of NAPE-PLD expression were observed by injecting the TRPV1 antagonist I-RTX and URB597 into the IC of NP rats. We can infer from the results that the activity of TRPV1 induced the synthesis of NAPE-PLD and promoted the production of AEA to produce analgesic effects.

Although there are limited studies on the cannabinoid signaling pathway in the IC, this region has been shown to be involved in processing pain signals. Furthermore, future work involving the measuring of AEA, PEA, OEA, or 2-AG levels in the context of FAAH inhibition may reinforce our results. We suggest CB2R, other TRP channel subfamilies, and COX-2 signaling be considered for future study to develop more effective pain control treatments. The current study provides insights on a potentially potent therapeutic target for managing NP and lays the groundwork for future studies to extend our understanding of NP.

In conclusion, this study shows that peripheral nerve injury-related neuropathy is linked to FAAH signals in the IC. Direct administration of URB597 to the IC inhibits allodynia and the excitation of neurons in the IC. These results suggest that URB597 may provide an alternative therapeutic target to modulate NP.

Authors' Contributions

MJK and BHL designed this study. MJK performed the immunostaining, immunoblotting, and behavioral experiments. MT provided the qPCR data. SWU performed the optical imaging.

MJK, MT, and SWU analyzed experimental data. SKH and BHL oversaw the experiments and edited the paper.

Declaration of Conflicting Interests

The author(s) declared no potential conflicts of interest with respect to the research, authorship, and/or publication of this article.

Funding

The author(s) disclosed receipt of the following financial support for the research, authorship, and/or publication of this article: This study was supported by the National Research Foundation of Korea grant funded by the Korea government (Ministry of Science and ICT) (NRF-2017R1A2B3005753).

ORCID iD

Bae Hwan Lee http://orcid.org/0000-0003-4719-9021

References

1. Campbell JN and Meyer RA. Mechanisms of neuropathic pain. *Neuron* 2006; 52: 77–92.
2. Attal N, Cruccu G, Baron R, Haanpää M, Hansson P, Jensen TS and Nurmikko T. EFNS guidelines on the pharmacological treatment of neuropathic pain: 2010 revision. *Eur J Neurol* 2010; 17: 1113–e1188.
3. Finnerup NB, Haroutounian S, Kamerman P, Baron R, Bennett DLH, Bouhassira D, Cruccu G, Freeman R, Hansson P, Nurmikko T, Raja SN, Rice ASC, Serra J, Smith BH, Treede R-D and Jensen TS. Neuropathic pain: an updated grading system for research and clinical practice. *Pain* 2016; 157: 1599–1606.
4. Attal N, de Andrade DC, Adam F, Ranoux D, Teixeira MJ, Galhardoni R, Raicher I, Üçeyler N, Sommer C and Bouhassira D. Safety and efficacy of repeated injections of botulinum toxin A in peripheral neuropathic pain (BOTNEP): a randomised, double-blind, placebo-controlled trial. *Lancet Neurol* 2016; 15: 555–565.
5. Han J, Kwon M, Cha M, Tanioka M, Hong S-K, Bai SJ and Lee BH. Plasticity-related PKMzeta signaling in the insular cortex is involved in the modulation of neuropathic pain after nerve injury. *Neural Plasticity* 2015; 2015: 601767.
6. Coghill RC, Talbot JD, Evans AC, Meyer E, Gjedde A, Bushnell MC and Duncan GH. Distributed processing of pain and vibration by the human brain. *J Neurosci* 1994; 14: 4095–4108.
7. Ploghaus A, Tracey I, Gati JS, et al. Dissociating Pain from Its Anticipation in the Human Brain. *Science (New York, NY)* 1999; 284: 1979–1981.
8. Peyron R, Schneider F, Faillenot I, Convers P, Barral F-G, Garcia-Larrea L and Laurent B. An fMRI study of cortical representation of mechanical allodynia in patients with neuropathic pain. *Neurology* 2004; 63: 1838–1846.
9. Berthier M, Starkstein S and Leiguarda R. Asymbolia for pain: a sensory-limbic disconnection syndrome. *Ann Neurol* 1988; 24: 41–49.
10. Benison AM, Chumachenko S, Harrison JA, Maier SF, Falci SP, Watkins LR and Barth DS. Caudal granular insular cortex is sufficient and necessary for the long-term maintenance of allodynic behavior in the rat attributable to mononeuropathy. *J Neurosci* 2011; 31: 6317–6328.
11. Coffeen U, Manuel Ortega-Legaspi J, Lopez-Munoz FJ, et al. Insular cortex lesion diminishes neuropathic and inflammatory pain-like behaviours. *Eur J Pain (London, England)* 2011; 15: 132–138.
12. Starr CJ, Sawaki L, Wittenberg GF, Burdette JH, Oshiro Y, Quevedo AS and Coghill RC. Roles of the insular cortex in the modulation of pain: insights from brain lesions. *J Neurosci* 2009; 29: 2684–2694.
13. Gaoni Y and Mechoulam R. Isolation, structure, and partial synthesis of an active constituent of hashish. *J Am Chem Soc* 1964; 86: 1646–1647.
14. Pertwee RG. Ligands that target cannabinoid receptors in the brain: from THC to anandamide and beyond. *Addict Biol* 2008; 13: 147–159.
15. Pertwee RG. The therapeutic potential of drugs that target cannabinoid receptors or modulate the tissue levels or actions of endocannabinoids. *AAPS J* 2005; 7: E625–E654.
16. Matsuda LA, Lolait SJ, Brownstein MJ, Young AC and Bonner TI. Structure of a cannabinoid receptor and functional expression of the cloned cDNA. *Nature* 1990; 346: 561–564.
17. Munro S, Thomas KL and Abu-Shaar M. Molecular characterization of a peripheral receptor for cannabinoids. *Nature* 1993; 365: 61–65.
18. Pertwee RG. Cannabinoid receptors and pain. *Prog Neurobiol* 2001; 63: 569–611.
19. Howlett AC, Barth F, Bonner TI, et al. International Union of Pharmacology. XXVII. Classification of cannabinoid receptors. *Pharmacol Rev* 2002; 54: 161–202.
20. Pertwee RG and Ross RA. Cannabinoid receptors and their ligands. *Prostaglandins Leukot Essent Fatty Acids* 2002; 66: 101–121.
21. Wotherspoon G, Fox A, McIntyre P, Colley S, Bevan S and Winter J. Peripheral nerve injury induces cannabinoid receptor 2 protein expression in rat sensory neurons. *Neuroscience* 2005; 135: 235–245.
22. Ross RA, Coutts AA, McFarlane SM, Anavi-Goffer S, Irving AJ, Pertwee RG, MacEwan DJ and Scott RH. Actions of cannabinoid receptor ligands on rat cultured sensory neurones: implications for antinociception. *Neuropharmacology* 2001; 40: 221–232.
23. Pertwee RG. *Cannabinoids [Handbook of Experimental Pharmacology]*. Vol. 168. Berlin, Germany: Springer, 2005.
24. Mechoulam R, Ben-Shabat S, Hanus L, Ligumsky M, Kaminski NE, Schatz AR, Gopher A, Almog S, Martin BR, Compton DR, Pertwee RG, Griffin G, Bayewitch M, Barg J and Vogel Z. Identification of an endogenous 2-monoglyceride, present in canine gut, that binds to cannabinoid receptors. *Biochem Pharmacol* 1995; 50: 83–90.
25. Sugiura T, Kondo S, Sukagawa A, Nakane S, Shinoda A, Itoh K, Yamashita A and Waku K. 2-Arachidonoylgylcerol: A possible endogenous cannabinoid receptor ligand in brain. *Biochem Biophys Res Commun* 1995; 215: 89–97.

26. Devane W, Hanus L, Breuer A, Pertwee R, Stevenson L, Griffin G, Gibson D, Mandelbaum A, Etinger A and Mechoulam R. Isolation and structure of a brain constituent that binds to the cannabinoid receptor. *Science* 1992; 258: 1946–1949.
27. Tzavara ET, Li DL, Moutsimilli L, Bisogno T, Di Marzo V, Phebus LA, Nomikos GG and Giros B. Endocannabinoids activate transient receptor potential vanilloid 1 receptors to reduce hyperdopaminergia-related hyperactivity: therapeutic implications. *Biol Psychiatry* 2006; 59: 508–515.
28. Chiou L-C, Hu SS-J and Ho Y-C. Targeting the cannabinoid system for pain relief? *Acta Anaesthesiol Taiwan* 2013; 51: 161–170.
29. Di Marzo V, De Petrocellis L and Bisogno T. The biosynthesis, fate and pharmacological properties of endocannabinoids. *Handb Exp Pharmacol* 2005; 147–185.
30. Sugiura T and Waku K. Cannabinoid receptors and their endogenous ligands. *J Biochem* 2002; 132: 7–12.
31. Di Marzo V. The endocannabinoid system: its general strategy of action, tools for its pharmacological manipulation and potential therapeutic exploitation. *Pharmacol Res* 2009; 60: 77–84.
32. Richardson JD, Aanonsen L and Hargreaves KM. Antihyperalgesic effects of spinal cannabinoids. *Eur J Pharmacol* 1998; 345: 145–153.
33. Helyes Z, Nemeth J, Than M, et al. Inhibitory effect of anandamide on resiniferatoxin-induced sensory neuropeptide release in vivo and neuropathic hyperalgesia in the rat. *Life Sci* 2003; 73: 2345–2353.
34. Rahn EJ and Hohmann AG. Cannabinoids as pharmacotherapies for neuropathic pain: from the bench to the bedside. *Neurotherapeutics* 2009; 6: 713–737.
35. Lichtman AH, Leung D, Shelton CC, et al. Reversible inhibitors of fatty acid amide hydrolase that promote analgesia: evidence for an unprecedented combination of potency and selectivity. *J Pharmacol Exp Ther* 2004; 311: 441–448.
36. Kinsey SG, Long JZ, O'Neal ST, Abdullah RA, Poklis JL, Boger DL, Cravatt BF and Lichtman AH. Blockade of endocannabinoid-degrading enzymes attenuates neuropathic pain. *J Pharmacol Exp Ther* 2009; 330: 902–910.
37. Leung D, Saghatelian A, Simon GM and Cravatt BF. Inactivation of N-Acyl phosphatidylethanolamine phospholipase D reveals multiple mechanisms for the biosynthesis of endocannabinoids. *Biochemistry* 2006; 45: 4720–4726.
38. Paxinos G and Watson C. *The rat brain in stereotaxic coordinates*. London, UK: Academic Press, 2007.
39. Han J, Cha M, Kwon M, Hong S-K, Bai SJ and Lee BH. In vivo voltage-sensitive dye imaging of the insular cortex in nerve-injured rats. *Neurosci Lett* 2016; 634: 146–152.
40. Lee BH, Won R, Baik EJ, Lee SH and Moon CH. An animal model of neuropathic pain employing injury to the sciatic nerve branches. *Neuroreport* 2000; 11: 657–661.
41. Yesilyurt O, Cayirli M, Sakin YS, Seyrek M, Akar A and Dogrul A. Systemic and spinal administration of FAAH, MAGL inhibitors and dual FAAH/MAGL inhibitors produce antipruritic effect in mice. *Arch Dermatol Res* 2016; 308: 335–345.
42. Mitrirattanakul S, Ramakul N, Guerrero AV, Matsuka Y, Ono T, Iwase H, Mackie K, Faull KF and Spigelman I. Site-specific increases in peripheral cannabinoid receptors and their endogenous ligands in a model of neuropathic pain. *Pain* 2006; 126: 102–114.
43. Horvath G, Kekesi G, Nagy E and Benedek G. The role of TRPV1 receptors in the antinociceptive effect of anandamide at spinal level. *Pain* 2008; 134: 277–284.
44. Gussew A, Rzanny R, Erdtel M, Scholle HC, Kaiser WA, Mentzel HJ and Reichenbach JR. Time-resolved functional 1H MR spectroscopic detection of glutamate concentration changes in the brain during acute heat pain stimulation. *NeuroImage* 2010; 49: 1895–1902.
45. Frot M, Faillenot I and Mauguiere F. Processing of nociceptive input from posterior to anterior insula in humans. *Hum Brain Mapp* 2014; 35: 5486–5499.
46. Hama AT, Germano P, Varghese MS, Cravatt BF, Milne GT, Pearson JP and Sagen J. Fatty acid amide hydrolase (FAAH) inhibitors exert pharmacological effects, but lack antinociceptive efficacy in rats with neuropathic spinal cord injury pain. *PloS One* 2014; 9: e96396.
47. Peng X, Studholme K, Kanjiya MP, et al. Fatty-acid-binding protein inhibition produces analgesic effects through peripheral and central mechanisms. *Mol Pain* 2017; 13: 1744806917697007.
48. Soukupova M, Palazzo E, De Chiaro M, et al. Effects of URB597, an inhibitor of fatty acid amide hydrolase (FAAH), on analgesic activity of paracetamol. *Neuro Endocrinol Lett* 2010; 31: 507–511.
49. Kwon M, Han J, Kim UJ, et al. Inhibition of mammalian target of rapamycin (mTOR) signaling in the insular cortex alleviates neuropathic pain after peripheral nerve injury. *Front Mol Neurosci* 2017; 10: 79.
50. Ploghaus A, Tracey I, Gati JS, Clare S, Menon RS, Matthews PM and Rawlins JN. Dissociating pain from its anticipation in the human brain. *Science* 1999; 284: 1979–1981.
51. Coffeen U, Canseco-Alba A, Simón-Arceo K, Almanza A, Mercado F, León-Olea M and Pellicer F. Salvinorin A reduces neuropathic nociception in the insular cortex of the rat. *Eur J Pain* 2018; 22: 311–318.
52. Malek N, Mrugala M, Makuch W, Kolosowska N, Przewlocka B, Binkowski M, Czaja M, Morera E, Di Marzo V and Starowicz K. A multi-target approach for pain treatment: dual inhibition of fatty acid amide hydrolase and TRPV1 in a rat model of osteoarthritis. *Pain* 2015; 156: 890–903.
53. Nasirinezhad F, Jergova S, Pearson JP and Sagen J. Attenuation of persistent pain-related behavior by fatty acid amide hydrolase (FAAH) inhibitors in a rat model of HIV sensory neuropathy. *Neuropharmacology* 2015; 95: 100–109.
54. Seillier A, Dominguez Aguilar D and Giuffrida A. The dual FAAH/MAGL inhibitor JZL195 has enhanced effects on endocannabinoid transmission and motor behavior in rats as compared to those of the MAGL inhibitor JZL184. *Pharmacol Biochem Behav* 2014; 124: 153–159.
55. Chae Y, Park H-J, Hahm D-H, Lee B-H, Park H-K and Lee H. Spatiotemporal patterns of neural activity in

response to electroacupuncture stimulation in the rodent primary somatosensory cortex. *Neurol Res* 2010; 32: 64–68.
56. Gao YJ and Ji RR. c-Fos and pERK, which is a better marker for neuronal activation and central sensitization after noxious stimulation and tissue injury? *Open Pain J* 2009; 2: 11–17.
57. Santos PL, Brito RG, Matos J, et al. Fos protein as a marker of neuronal activity: a useful tool in the study of the mechanism of action of natural products with analgesic activity. *Mol Neurobiol* 2018; 55: 4560–4579.
58. Starowicz K, Makuch W, Korostynski M, Malek N, Slezak M, Zychowska M, Petrosino S, De Petrocellis L, Cristino L, Przewlocka B and Di Marzo V. Full inhibition of spinal FAAH leads to TRPV1-mediated analgesic effects in neuropathic rats and possible lipoxygenase-mediated remodeling of anandamide metabolism. *PloS One* 2013; 8: e60040.
59. Pertwee RG. The diverse CB(1) and CB(2) receptor pharmacology of three plant cannabinoids: Δ(9)-tetrahydrocannabinol, cannabidiol and Δ(9)-tetrahydrocannabivarin. *Br J Pharmacol* 2008; 153: 199–215.
60. Zhuo M. Central plasticity in pathological pain. *Novartis Found Symp* 2004; 261: 132–145; discussion 145–154.
61. Zhuo M. Contribution of synaptic plasticity in the insular cortex to chronic pain. *Neuroscience* 2016; 338: 220–229.
62. Maggio N, Shavit Stein E and Segal M. Cannabidiol regulates long term potentiation following status epilepticus: mediation by calcium stores and serotonin. *Front Mol Neurosci* 2018; 11: 32.
63. Silva-Cruz A, Carlström M, Ribeiro JA and Sebastião AM. Dual influence of endocannabinoids on long-term potentiation of synaptic transmission. *Front Pharmacol* 2017; 8: 921.
64. Jayamanne A, Greenwood R, Mitchell VA, Aslan S, Piomelli D and Vaughan CW. Actions of the FAAH inhibitor URB597 in neuropathic and inflammatory chronic pain models. *Br J Pharmacol* 2006; 147: 281–288.
65. Kinsey SG, Long JZ, O'Neal ST, Abdullah RA, Poklis JL, Boger DL, Cravatt BF and Lichtman AH. Blockade of endocannabinoid-degrading enzymes attenuates neuropathic pain. *J Pharmacol Exp Ther* 2009; 330: 902–910.
66. Centonze D, Bari M, Rossi S, Prosperetti C, Furlan R, Fezza F, De Chiara V, Battistini L, Bernardi G, Bernardini S, Martino G and Maccarrone M. The endocannabinoid system is dysregulated in multiple sclerosis and in experimental autoimmune encephalomyelitis. *Brain* 2007; 130: 2543–2553.
67. Bishay P, Schmidt H, Marian C, Häussler A, Wijnvoord N, Ziebell S, Metzner J, Koch M, Myrczek T, Bechmann I, Kuner R, Costigan M, Dehghani F, Geisslinger G and Tegeder I. R-flurbiprofen reduces neuropathic pain in rodents by restoring endogenous cannabinoids. *PloS One* 2010; 5: e10628.
68. Fegley D, Gaetani S, Duranti A, et al. Characterization of the fatty acid amide hydrolase inhibitor cyclohexyl carbamic acid 3′-carbamoyl-biphenyl-3-yl ester (URB597): effects on anandamide and oleoylethanolamide deactivation. *J Pharmacol Exp Ther* 2004; 313: 352–358.
69. Pertwee RG. Ligands that target cannabinoid receptors in the brain: from THC to anandamide and beyond. *Addict Biol* 2008; 13: 147–159.
70. Toth A, Boczan J, Kedei N, et al. Expression and distribution of vanilloid receptor 1 (TRPV1) in the adult rat brain. *Brain Res Mol Brain Res* 2005; 135: 162–168.
71. Kathuria S, Gaetani S, Fegley D, Valiño F, Duranti A, Tontini A, Mor M, Tarzia G, Rana GL, Calignano A, Giustino A, Tattoli M, Palmery M, Cuomo V and Piomelli D. Modulation of anxiety through blockade of anandamide hydrolysis. *Nat Med* 2003; 9: 76–81.